Wear 274–275 (2012) 68–74

Contents lists available at ScienceDirect

Wear

journal homepage: www.elsevier.com/locate/wear

In-service behaviour of (Ti,Si,Al)N_x nanocomposite films

S. Carvalho[a,*], N.M.G. Parreira[b], M.Z. Silva[a], A. Cavaleiro[b], L. Rebouta[a]

[a] Centro de Física (GRF), Universidade do Minho, Campus de Azurém, 4800-058 Guimarães, Portugal
[b] SEG-CEMUC Mechanical Engineering Department, University of Coimbra, 3030-788 Coimbra, Portugal

ARTICLE INFO

Article history:
Received 22 November 2010
Received in revised form 20 July 2011
Accepted 8 August 2011
Available online 1 September 2011

Keywords:
Self hardening
Cutting tools
Wear
Oxidation resistance
Lubricious oxides

ABSTRACT

This paper reports on the optimization of (Ti,Si,Al)N_x coatings to improve the performance of coated tools in dry cutting applications. The performance and the wear mechanisms of (Ti,Si,Al)N_x tungsten carbide coated tools were investigated. Tool life and tool failure modes were thoroughly examined by scanning electron microscopy (SEM) complemented with energy dispersive spectroscopy (EDS) in order to study the wear mechanisms. After 15 min at high cutting speed (200 m/min), the cutting edges of almost all the coatings still remained in good conditions. The results presented on this paper confirmed that nc-($Ti_{1-x}Al_x$)/a-SiN_x nanocomposite coatings offer a significant potential to operate in extreme environments, since this coating outperformed one of the best solutions actually available in the market for high speed turning. An improvement on the tribological behaviour of (Ti,Si,Al)N_x films was also observed with thermal annealing before the turning tests, due to a self hardening effect as consequence of the spinodal segregation of the (Ti,Al,Si)N metastable phase. On the other hand, no significative increase on the performance of the coated tools was observed with depositing an amorphous Al_2O_3 interlayer.

1. Introduction

The demand on the improvement of machining technology, in terms of higher cutting speed, better quality of the machined surface, lower consumption of lubricants and coolants, calls for the development of new wear resistant coatings. While superhard coatings show quite notable behaviour for the protection of cutting tools, most tribological applications using coatings require either high toughness or low friction coefficient and low wear rate. Designs for tough wear protective coatings are roughly divided into three categories: multilayers, functional gradients and nanocomposite [1–4]. Recently hard coatings have been still developed in order to increase the machining speed, the lifetime of the coated tools and to improve the quality of the machined surface [5–10]. However, there is still a large potential for improving the presently manufactured high-performance coatings. Previous research work with (Ti,Si,Al)N_x system demonstrated that the deposited films could belong to either the class of nanocomposite or multilayer materials depending on the deposition rate is lower or higher than 2 μm/h, respectively [11–13]. As discussed on [13], further improvements of the wear resistance of (Ti,Si,Al)N_x films could be expected by:

(i) Increasing Si content to values higher than 4 at.%.
(ii) Using thermal annealing in vacuum before the turning tests in order to relax the internal stresses.

The objective of the present work is to fulfil these two points and to study the effect of an Al_2O_3 interlayer on the mechanical performance of (Ti,Si,Al)N_x films. In fact, it seems that the wear resistance results from a specific favourable combination of hardness and toughness which is sometimes difficult to be achieved with a single coating [14]. For example, a WC–TiC–TiN (outside layer) graded coating for cutting tools was reported by Fella et al. [15], which showed considerable less wear than single layer hard coatings used in the cutting of steels. Based on these ideas, an aluminium oxide layer, which possesses a good thermal shock resistance and usually adhesion strength to the substrate [16], was deposited between the substrate (WC-Co) and the (Ti,Si,Al)N_x coating. It was expected a gradual build-up material hardness from the substrate ($H \approx 16$ GPa) [17], crossing the Al_2O_3 ($H \approx 11$ GPa) [18] to the (Ti,Si,Al)N_x film ($H > 35$ GPa and $E > 350$ GPa) [19]. Also the Al_2O_3 between the coating and the substrate should provide thermal protection to this one and avoid the interdiffusion between the substrate and the (Ti,Si,Al)N_x top-coat.

2. Experimental details

2.1. Deposition and characterization of the coatings

(Ti,Si,Al)N_x coatings were deposited on WC-Co cemented carbide cutting tools and on stainless steel by reactive magnetron

* Corresponding author. Tel.: +351 253 510470; fax: +351 253 510461.
E-mail address: sandra.carvalho@fisica.uminho.pt (S. Carvalho).

0043-1648/$ – see front matter © 2011 Elsevier B.V. All rights reserved.
doi:10.1016/j.wear.2011.08.018

Table 1
Some experimental parameters, composition and mechanical properties relative to the sputtered samples. The applied Bias voltage was −70 V.

Tool	Ti (at. %)	Si (at. %)	Al (at.%)	N (at. %)	O (at. %)	Rate (μm/h)	H (GPa)	H^a (GPa)	E (GPa)	E^a (GPa)	Lc (N)	Interlayer
CP1	29.2	5.5	9.3	51	5	0.8	9 ± 2	8 ± 1	338 ± 80	332 ± 33	19	TiAlSi (0.35 μm) + Al_2O_3 (0.8 μm)
CP2	28.4	5.6	9	53	4	1.9	14 ± 6	14 ± 3	285 ± 48	264 ± 34	20	TiAlSi (0.35 μm) + Al_2O_3 (0.8 μm)
CP3	21	7	11	56	5	1.7	19 ± 5	21 ± 4	360 ± 17	298 ± 36	25	TiAlSi (0.35 μm)
P3[b]	41	4	7	48	–	1.6	29 ± 4	–	349 ± 78	–	–	TiAl (0.35 μm)

[a] After annealing at 800 °C.
[b] See elsewhere [13].

sputtering, in an Ar/N_2 atmosphere, using a custom made equipment. The system is composed of 4 unbalanced magnetrons cathodes vertically opposite, where a $Ti_{0.5}Al_{0.5}$ target and a pure Ti target incrusted with some Si pieces, and a pure Al target were placed leaving the fourth place as a decoy magnetron without a target. In order to change the composition of the samples, the current density applied to the (TiAl(Si) and Ti(Si)) magnetrons was varied in the range 10–15 mA cm^{-2}. An external heating resistance positioned at 80 mm from the substrate holder was used to heat the samples (300 °C), although the environmental temperature is more dependent on the deposition rate. Before the coatings deposition (with thicknesses ranging 2–4 μm), a TiAlSi adhesion layer was deposited in all samples and, in tools 1 and 2, also an Al_2O_3 interlayer (see Table 1). It should be pointed out that for each run, a plane SS and several WC-Co triangular tools (ISO TMNG 16 04 08-QM) were coated simultaneously. Some were tested as deposited without annealing in the lathe. Others, before turning tests, were subjected to a thermal cycle, in vacuum, consisting of a heating cycle of 1.5 h up to the annealing temperature (800 °C), 1 h hold at this temperature, followed by a slow cooling down to room temperature.

The atomic composition of the deposited samples was measured by electron probe microanalysis (EPMA) using a Cameca SX 50 apparatus. An average number of five "ball cratering" (BC) experiments were performed in each sample in order to determine its thickness. X-ray diffraction (XRD) experiments were performed, using a Cukα radiation, in order to study the coating's structure. The adhesion/cohesion of the coatings was evaluated by scratch-testing technique, using a Revetest apparatus from CSM Instruments. The load was increased linearly from 0 to 50 N (Rockwell C 200 μm radius indenter tip, loading speed of 100 N/min, and scratch speed of 10 mm/min). The critical load (Lc) values corresponding to the different failure mechanisms (adhesive/cohesive) were measured by analyzing the failures events in the scratch track, by optical microscopy.

The hardness was evaluated by depth-sensing indentation, using a Fisherscope H100 equipment at maximum load of 40 mN. Correction of the geometrical defects in the tip of the indenter, thermal drift of the equipment and uncertainty of the initial contact was considered [20–22] It should be point out that all these previous measurements were carried out on the coatings deposited on the WC-Co cemented carbide cutting tools, exception the residual stress measurements which were studied in the samples deposited at the same time as the coated tools, on stainless steel (AISI 316). So, the residual stresses, σ_r, were obtained by the deflection method from the Stoney's equation [23], using substrate curvature radii, both before and after coating deposition [24]. In fact, these stress results cannot be analysed as absolute values but only in comparative behaviour between the samples.

2.2. In service behaviour: turning tests

A Cincinnati Milacron Hawk-150 numerically controlled lathe was used to perform the machining experiments. These turning tests were performed in different machining conditions, using steel as working material. The selected steel was an usual commercial alloy steel (30-CrNiMo8 – W nr. 1.6580 by DIN EN 100083-1), with a hardness value of 3.8 GPa. The tests were performed for each sample three times on different edges and with new tools for v = 200 m/min and f_n = 0.1 mm/rev, in dry turning conditions. In fact, by eliminating the coolant the amount of heat generated at the cutting zone increases, creating the potential for the premature tool wear. Consequently, severe conditions of machining were better simulated in this way. Meanwhile, the environmentally friendly recycling and disposal of the coolants represents 15–30% of the total machining cost [25]. The following conventional tool wear parameters were measured by Scanning Electron Microscopy (SEM): V_B – maximum flank wear, KM – distance between the tool edge and the crater centre (rake face). After the turning tests, the dominant wear mechanisms were revealed by morphological observation and chemical modification analysis was also performed in the SEM, which was equipped with an Energy Dispersive X-ray Spectrometry (EDS). The commercial cutting tool (using for comparison) was produced by CVD; the coating comprised a 8.8 μm Ti(C,N) base layer, a 4.3 μm intermediate Al_2O_3 layer and a 1.6 μm top TiN layer, with 22 GPa as hardness.

3. Results

3.1. Chemical and structural analysis

A summary of the coatings properties under investigation in this work is presented in Table 1. The differences in the composition of the various samples, as well as in the deposition rate are related with the current density applied to both magnetron cathodes (TiAl(Si)) and Ti(Si)). Approximately 5 at.% of oxygen was detected in all coatings, which is related with the base pressure. It should be point out that Si contents higher than 4 at. % were reached as desired and discussed on [13]. XRD experiments showed that in all coatings the f.c.c structure with (1 1 1) texture (see e.g., Fig. 1a),

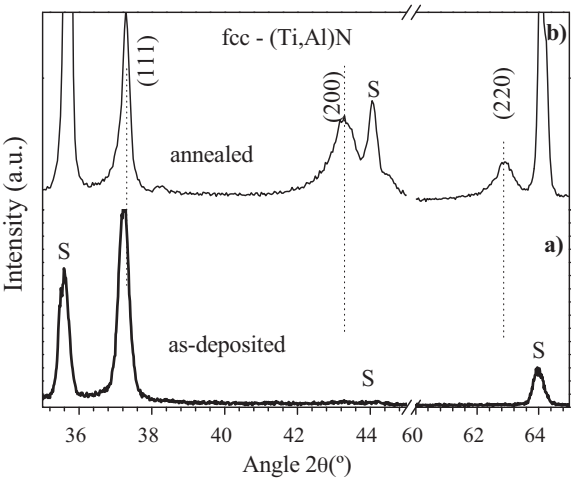

Fig. 1. (a) XRD pattern of CP3 film as-deposited. (b) XRD pattern of CP3 film after been annealed in vacuum at 800 °C.

similar to TiN, was developed, as discussed in several previous works [19,26,27].

XRD scans (see Fig. 1b) from CP3 coating annealed at 800 °C, show the development of new small broad peaks (2 0 0) and (2 2 0), which can be assigned to crystalline fcc–(Ti,Al)N. The broad peaks shows that those grains have a small size, and result from spinodal segregation of the (Ti,Al,Si)N metastable phase with the thermal annealing [28]. This is supported by the hardness increase, as it will be shown in the next section. Thus, this also demonstrates that a metastable phase was formed in the as-deposited samples, due to the low deposition temperature. More detailed studies and further characterization of nc-$(Al_{1-x}Ti_x)N$/a-Si_3N_4 nanocomposite coatings after at high-temperatures decomposition is well discussed by Veprek et al. on [29,30]

3.2. Mechanical properties

The hardness (H) and Young's modulus (E) of the samples before and after thermal annealing are presented in Table 1. No significant changes on the hardness values are observed after annealing at 800 °C, except a small increase in the hardness values of the CP3 coating, which can be related with self hardening effects [31–34].

This behaviour suggests that the increase of the hardness upon annealing is associated with a partial stabilization of the nanostructure nc-$Ti_{1-x}Al_x$/a-SiN_x, which occurs due to a transformation by spinodal segregation.

It is possible to observe that all the samples present values much lower than the typical values reported for $(Ti,Si,Al)N_x$ coatings [13]. This behaviour should be firstly related with the low deposition temperature [33] and with the O amount present in the films. In fact, Vepřěk et al. [35] noticed that the hardness in nc-TiN/a-SiN_x nanocomposites is strongly degraded at oxygen impurity concentrations higher than 0.1 at.%.

The film-to-substrate adhesion is extremely critical to achieve longer wear life or durability, especially on the surfaces of tribomaterials [36]. The values for the critical adhesion loads, Lc, corresponding to the first adhesive failures are shown in Table 1. For all coatings, the critical load for the first adhesive failure varied between 19 and 25N. The values obtained for samples CP1 and CP2 are close to 20 N, whereas for sample CP3 is around 25 N. In the case of the deposition with an interlayer, the adhesion between the interlayer and the coatings is also a very important parameter. Using an optical microscope is very difficult to identify if the failure occurs at the substrate/interlayer or interlayer/ coating interfaces. However the idea for introducing an interlayer was to improve the adhesion and it was found that the critical load obtained for TiSiAl layer on substrate was higher than 50 N. Hence, for the $(Ti,Si,Al)N_x$ coatings the observed failure should occur mainly in the interlayer/coating interface. The better behaviour of the sample CP3 in comparison to the others seems to be only attributed to the inexistence of the Al_2O_3 interlayer. The coating deposited without Al_2O_3 layer has higher critical load because in this coating the variation between the substrate and the film is less abrupt, as it is when an Al_2O_3 layer is added.

3.3. Cutting performance

3.3.1. Wear evaluation: flank and rake wear

The cutting performance of the coated tools during turning alloy steel was evaluated considering the average of the maximum flank (VB) and the rake (KM) wears (see Table 2). For comparison purposes, Table 2 presents also the wear parameters for the best $(Ti,Si,Al)N_x$ coated tool – P3, tested previously in the same conditions [13], and for a commercial multilayer coating ($TiCN/Al_2O_3/TiN$) deposited by CVD, that is widespread used in the market, which will be treated as the reference for this work.

For the same machining time (15 min) in the same cutting conditions, it was observed that:

(i) CP1 tool showed a premature failure due to the very high values of flank and rake wears. Several factors could explain this bad behaviour: first the presence of the Al_2O_3 layer; second the low thickness value (<2 μm) and the oxygen content on the film. Another possible reason should be related with the high residual stress values, observed for this sample (-3.0 ± 0.47 GPa), since this sample was deposited with low deposition rate and consequently low deposition temperature. The CP3 and CP2 samples showed only -1 ± 0.09 GPa for compressive residual stresses. It is however worth to notice that these stress values should be seen only a variation tendency, since different substrates were used for their evaluation.

(ii) The flank (VB) and rake (KM) are values that are significantly lower for the CP3 tool, when compared with the wear parameters presented by the commercial insert and by the other tools.

(iii) The rake wear (KM) values of the commercial and CP2 tools are comparable. Anyway, the flank wear (VB) is significantly higher for the CP2 tool. This difference in the performance of the tools should be related with the chip behaviour. In the tests with the commercial tool, the chips from the machining process were in the form of small fragments (as also observed with CP3 tool), while for the CP2 tool the chip wound around the tool, which contributed for the heating of the tool tip. The extreme heating of the cutting edge, may enhance thermal cracks and consequently originate premature failures in the tool surface, as is well discussed on [37]. This chip behaviour is sometimes related with the cutting edge roundness. The effective radius of the cutting edge tip consists of the radius of the WC-Co insert plus the coating, which follows the curvature of the substrate during the deposition process. And in fact the CP2 thickness (4.2 μm) is slightly higher than the CP3 (3.7 μm).

(iv) Slightly superior wear behaviour of the annealed coated inserts compared with the not annealed ones was visible, also due to the self hardening effects, which occurs due to spinodal decomposition of $(Ti,Al,Si)N_x$.

(v) Concerning the tool life, the most noticeable fact is that for similar turning conditions the CP3 tool showed a promising behaviour, comparing with the commercial tool.

3.3.2. Wear mechanisms

Before the turning tests, a detailed study of the chemical composition variation throughout the edge was performed by EDS on several points of the tool. Fig. 2 presents the EDS results for points located 0.05 mm (Fig. 2a), 0.4 mm (Fig. 2b) and 1 mm (Fig. 2c) from the top of the edge. The evolution of chemical composition obtained from the EDS of Fig. 2a–c is represented in Fig. 2d. The analysis of these figures shows that there is no significant gradient on the composition (for as-deposited samples, before cutting tests) from the top edge down to 0.4 mm, and only a small variation can be visible for the highest distances (>1.0 mm). Thus, if any variation on the composition is detected in the 0.4 mm range, it should be related with the turning tests and with the tool behaviour when tested at elevated temperatures.

The micrographs in Figs. 3–6 illustrate the changes in rake and flank wear patterns of the tools after machining during 15 min at $v = 200$ m/min. In all the worn zones of the tested tools, iron contamination coming from the workpiece was detected (EDS A in all figures). On the worn surface of CP2 tool (not annealed) (Fig. 3), only minor traces of wear along the rake face (inset B) and significant surface damage in the flank face (inset C) are observed. Also, the zone A shows a "brushing-off" of debris. The SEM micrograph

Table 2
Tool wear data after turning 15 min with $v = 200$ m/min and fn = 0.1 mm/rev.

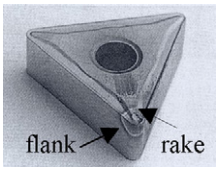

	Results for tools without annealing			Results for tools with annealing at 800 °C			Tool life (min)
	KM (μm)	VB (μm)	SEM micrographs	KM (μm)	VB (μm)	SEM micrographs	
CP1	Tool breakage	Tool breakage	–	–	–	–	–
CP2	180	575	Fig. 2	180	308	Fig. 3	–
CP3	80	30	Fig. 4	70	22	Fig. 5	45
P3	192	47	–	–	–	–	33
Commercial	157	50	–	–	–	–	42

of the crater wear of CP2 cutting tool with annealing is illustrated in Fig. 4. Significant surface damage in the form of adhered and scratch appearance can be seen on the rake face. This suggests that the primary wear mechanisms are abrasive and adhesive wear. For this sample, a pronounced crater was formed and, in some areas of the tool, complete wear throughout the coating until the substrate was also observed (EDS B in Fig. 4).

SEM micrographs of the crater wear track of CP3 tool not annealed (Fig. 5) and after annealing at 800 °C (Fig. 6) show no significant wear.

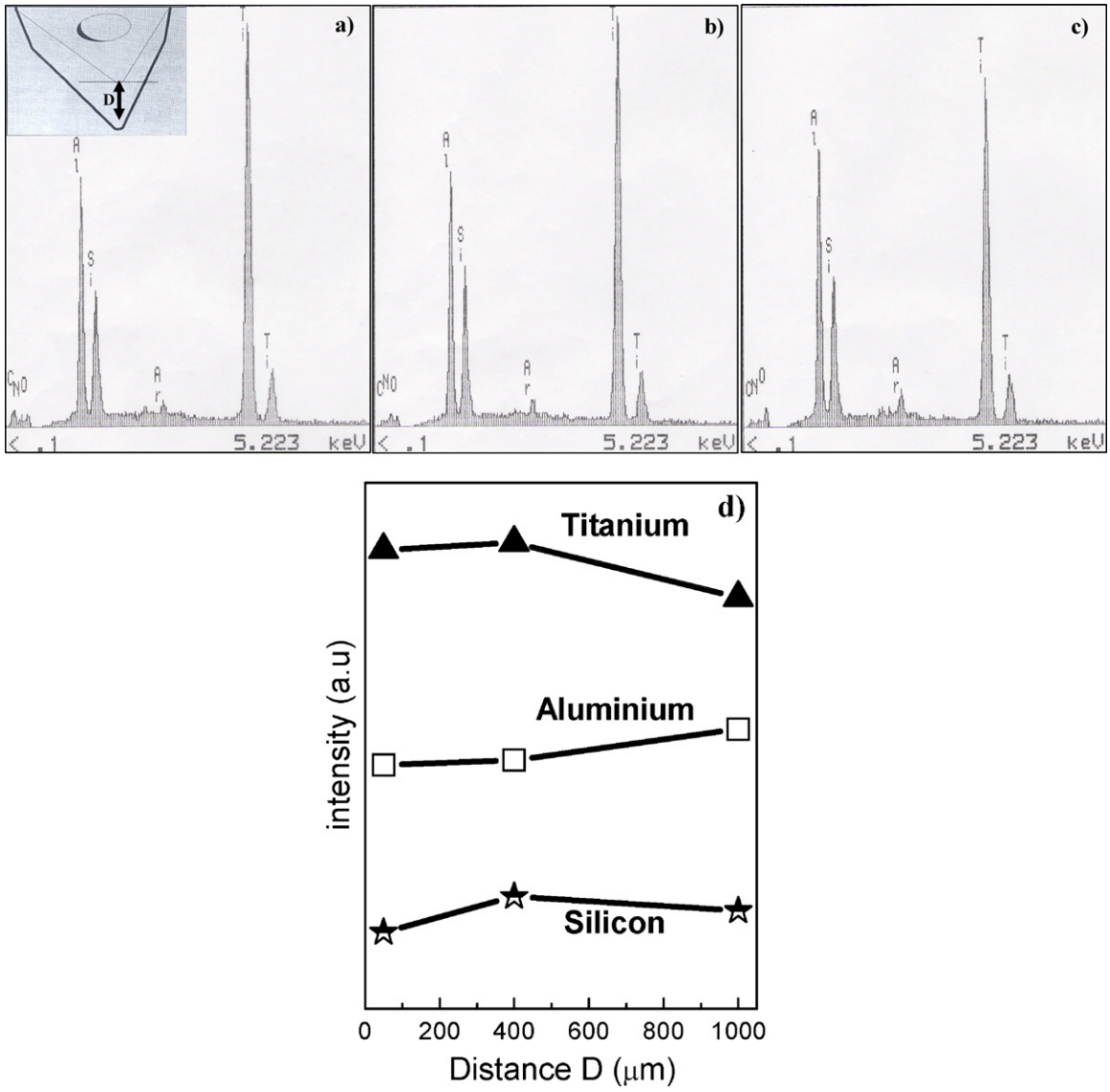

Fig. 2. EDS analysis for three different points on the tool edge. (a) $D = 0.05$ mm, (b) $D = 0.4$ mm, (c) $D = 1$ mm, and (d) chemical composition on several points of the tool.

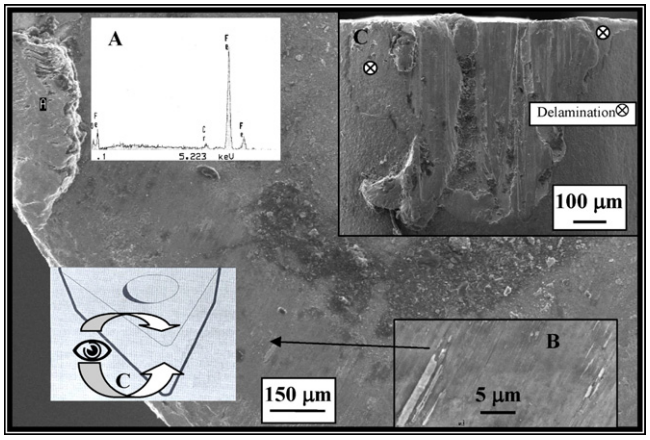

Fig. 3. Crater wear of the CP2 tool after machining 15 min at V_c = 200 m/min. The EDS (A) analysis on the worn region indicates adhesion of the work material (Fe) onto the rake face of the tool. Inset (B): amplification of the rake face wear, showing numerous scratches. Inset (C): SEM image of the flank face wear, showing coating delamination.

4. Discussion

It is recognised that hardness is not necessarily the prime requirement for wear resistance, and it is known that commercial coating solutions using soft materials, such as self-lubricant coatings, MoS_2 or WS_2 can be an excellent alternative for wear protection [38–40]. In this work the hardness values were lower than expected, however the aforementioned cutting tests proved that the (Ti,Si,Al)N_x coating (CP3 sample) outperformed one of the best solutions actually available in the market for high speed turning.

The first important point to be taken into account is the possible self hardening process occurring during the turning tests. This structural transformation resulted not only in a hardness increase but, more important in a significant decrease on the Young's modulus. It was already recognised by several authors that the ratio between H and E, the so-called "plasticity index", is widely quoted as a valuable measure in determining the limit of the elastic behaviour in the surface contact, which is clearly an important parameter to avoid wear [38].

The second parameter is related to the fact that the CP3 coating, when tested at elevated temperatures, can effectively retard the abrasive and oxidation wear owing to the formation of a resistant

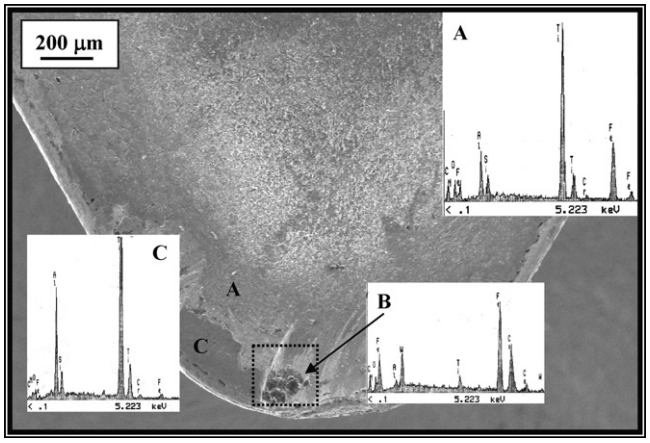

Fig. 4. Rake wear of the CP2 tool (annealed) after machining 15 min at V_c = 200 m/min. The EDS (A) analysis on the worn region and inset B (amplification of the rake face wear) indicates adhesion of the work material (Fe) onto the rake face of the tool. EDS (B) analysis indicates that the coating has been removed. EDS (C) analysis indicates that the coating has not been completely removed.

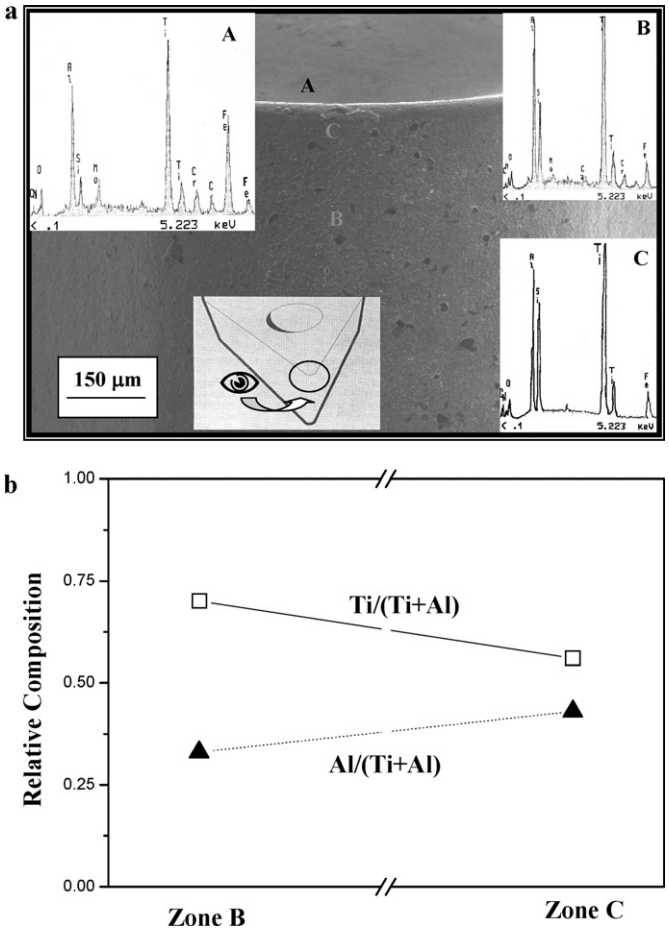

Fig. 5. SEM image of tool CP3 after cutting 15 min at V_c = 200 m/min, showing mainly the flank face wear. The EDS (A) analysis on the worn region indicates adhesion or welding of the work material onto the rake face of the tool. EDS (B and C) analysis indicates that the coating has not yet been removed on the flank. EDS (B) denounces the formation of an oxide layer (Al_2O_3). (b) Relative chemical composition of zone b and zone c from (a), for Ti and Al elements. The relative composition between Al and Ti indicate an enrichment of Al at coating surface.

oxide layer, which is supported by a hard coating. EDS results showed that, in some zones of the worn coated samples, oxygen is detected (EDS B in Fig. 5 and EDS on zone A in Fig. 6). When EDS B is compared with EDS C in Fig. 5 (see in more detail Fig. 5b), or when the relative chemical composition of zone B is compared with Zone C in Fig. 6 (see Fig. 6b), it shows an Al enrichment at the tool surface on the worn zone. The presence of oxygen (not always easy to detect by EDS) and the Al enrichment, suggests the formation of an Al_2O_3 layer, which should lead to a better oxidation resistance. This behaviour was already reported by Vaz et al. [41], on (Ti,Al)N system, where films growing with a (1 1 1) texture developed at high temperatures in air an oxide layered Al_2O_3–TiO_2 structure. According to these authors, this oxide layer protects the underlying nitride from further oxidation. This oxide layer also shows that the nanostructure is only partially stabilized, but also contributes for the improvement of the in-service behaviour of CP3 film. The role of Si in improving the oxidation resistance by the formation of the nanocomposite structure it is difficult to quantify, due to limitations mentioned in Section 3, but certainly had influence in the best performance of CP3 tool. In fact, in a previous work [13], it was observed a better cutting performance of the (Ti,Si,Al)N_x coatings comparing with (Ti,Al)N and it was also previously shown that $Ti_{0.27}Al_{0.53}Si_{0.2}N$ coating exhibited a better oxidation resistance at 900 °C than $Ti_{0.35}Al_{0.65}N$ coating. [41,42].

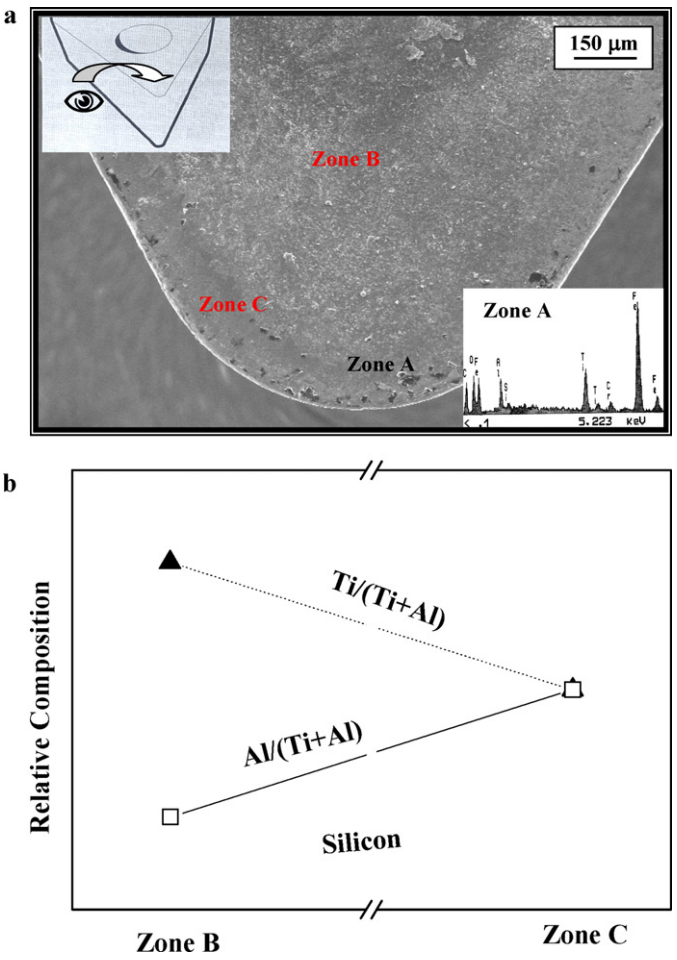

Fig. 6. (a) Rake wear of the CP3 annealed tool after machining 15 min at V_c = 200 m/min. The EDS analysis on the zone A indicates adhesion or welding of the work material onto the rake face of the tool. (b) Relative chemical composition of zone b and zone c from (a), for Ti and Al elements. The relative composition between Al and Ti indicate an enrichment of Al at coating surface.

Also, Veprek et al. [25] and Tanaka et al. [43] developed AlTiSiN coatings, which, showed an improved cutting performance, when compared to standard TiAlN and AlTiN coatings.

Besides the oxidation protector character of the oxide layers that can be formed during the turning tests, it should be also considered other beneficial aspects of the oxides concerning the tribological behaviour. Some papers were published where extremely low friction and/or low wear rates were attributed to some special oxide phases [44,45]. The self-formation of lubricious oxides on hard substrates lowered slightly the friction and/or considerably the wear. Ma et al. reported that due to the formation of a SiO_x layer, the friction coefficient of ternary Ti–Si–N coating was reduced from about 0.75 at room temperature to about 0.55 at 550 °C [46]. These results can also suggest that a mixed layer consisting of Al_2O_3 and TiO_2 could be responsible for low friction and low wear rate and, consequently, to the better cutting performance achieved for CP3 coating tool. Further tribological studies regarding the formation of these lubricious oxides should be performed on these samples, in order to quantify the apparent decrease on the friction coefficient or/and on the wear rate demonstrated by the CP3 tool, and clarify this point.

The results obtained with the Al_2O_3 interlayer did not reveal any improvement on the mechanical performance of (Ti,Si,Al)N_x nanocomposite films, probably due to a decrease of the adhesion, either between the layer or to the substrate. Such a fact can be confirmed by the coating delaminating observed by SEM on the flank wear of CP2 tool (insert C in Fig. 3). Besides, the Al_2O_3 deposited is amorphous with a featureless morphology, which is typical of fragile materials, giving rise to bad cutting properties.

5. Conclusions

In this study it was confirmed that nc-TiAlN/a-SiN_x nanocomposite coatings offer significant potential for operate in extreme environments, since one of the (Ti,Si,Al)N_x coating outperformed one of the best solutions actually available in the market for high speed turning. An age hardening processes during the turning tests, concomitantly with a decrease of the Young's modulus, gives rise to much higher H/E ratios which should be in the basis of the decrease in the wear rate. Furthermore, it was suggested that the formation of an Al_2O_3 layer improving the oxidation resistance and consequently the wear resistance. Furthermore, the possibility of the formation of lubricious oxides at the contact zone during wear can have a positive effect on tribological behaviour. The thermal annealing of the coated tools in vacuum before the turning tests must had induced a self hardening effect of coated tool, not compromising the coating-substrate adhesion, since for 200 m/min as cutting speed the wear parameters (the flank (VB) and rake (KM) wear values), after 15 min of turning test, decreased with thermal annealing.

Although the sample that presented the highest Si at.% showed the best in-service, the role of the Si at.% is not completely clarified but seems that the tribological behaviour should be correlated with the Al + Si/Ti ratio, and not only with the Si content! Nevertheless, the results obtained with Al_2O_3 an interlayer did not reveals an improvement on the mechanical performance of nanocomposite films.

References

[1] S. PalDey, S.C. Deevi, Single layer and multilayer wear resistant coatings of (Ti,Al)N: a review, Mater. Sci. Eng. 342 (2003) 58–79.
[2] A. Karimi, Y. Wang, T. Cselle, M. Morstein, Fracture mechanisms in nanoscale layered thin films, Thin Solid Films (2002) 275–280.
[3] A. Voevodin, J.S. Zabinski, C. Muratore, Recent advances in hard, tough and low friction nanocomposite coatings, Tsinghua Sci. Technol. 10 (6) (2005) 665–679.
[4] S. Vepřek, M.G.J. Vepřek-Heiman, P. Karvankova, Jan Prochazka, Different approaches to superhard coatings and nanocomposites, Thin Solid Films 476 (2005) 1–29.
[5] L. Settineri, M.G. Faga, G. Gautier, M. Perucca, Evaluation of wear resistance of AlSiTiN and AlSiCrN nanocomposite coatings for cutting tools, CIRP Ann. – Manuf. Technol. 57 (2008) 575–578.
[6] G.S. Fox-Rabinovich, J.L. Endrino, B.D. Beake, M. Kovalev, A. Gray, H. Aguirre, S.C. Veldhuis, D.T. Quinto, C.E.A.I. Bauer, Effect of temperature of annealing below 900 °C on structure, properties and tool life of an AlTiN coatings under various conditions, Surf. Coat. Technol. 202 (2008) 2985–2992.
[7] M. Sokovic, B. Barišić, S. Sladić, Model of quality management of hard coatings on ceramic cutting tools, J. Mater. Proc. Technol. 209 (2009) 4207–4216.
[8] F. Qin, Y.K. Chou, D. Nolen, R.G. Thompson, Coating thickness effects on diamond coated cutting tools, Surf. Coat. Technol. 204 (2009) 1056–1060.
[9] Y. Tang, Y.S. Li, Q. Yang, A. Hirose, Deposition and characterization of diamond coatings on WC-Co cutting tools with W/Al interlayer, Diamond Relat. Mater. 19 (2010) 496–499.
[10] M. Keunecke, C. Stein, K. Bewilogua, W. Koelker, D. Kassel, H. van den Berg, Modified TiAlN coatings prepared by d.c. pulsed magnetron sputtering, Surf. Coat. Technol. (2010), doi:10.1016/j.surfcoat.2010.09.023.
[11] S. Carvalho, F. Vaz, L. Rebouta, D. Schneider, A. Cavaleiro, E. Alves, Elastic properties of (Ti,Al,Si)N nanocomposite films, Surf. Coat. Technol. 142–144 (2001) 110–116.
[12] E. Ribeiro, A. Malczyk, S. Carvalho, L. Rebouta, J.V. Fernandes, E. Alves, A.S. Miranda, Effects of ion bombardment on properties of dc sputtered superhard (Ti, Si,Al)N nanocomposite coatings, Surf. Coat. Technol. 151–152 (2002) 515–520.
[13] S. Carvalho, E. Ribeiro, L. Rebouta, C. Tavares, J.P. Mendonça, A. Caetano Monteiro, N.J.M. Carvalho, M. J.Th. De Hosson, A. Cavaleiro, Microstructure, mechanical properties and cutting performance of superhard (Ti, SiAl)N nanocomposte films grown by dc reactive magnetron sputtering, Surf. Coat. Technol. 177–178 (2004) 459–468.

[14] M.T. Vieira, A.S. Ramos, The influence of ductile interlayers on the mechanical performance of tungsten nitride coatings, J. Mater. Proc. Technol. 92–93 (1999) 156–161.
[15] R. Fella, H. Holleck, H. Schulz, Preparation and properties of WC–TiC–TiN gradient coatings, Surf. Coat. Technol. 36 (1988) 257–264.
[16] X. Shi-Gang, S. Li-Xin, Z. Rong-Gen, H. Xing-Fang, Properties of aluminium oxide coating on aluminium alloy produced by micro-arc oxidation, Surf. Coat. Technol. 199 (2005) 184–188.
[17] H.C. Kim, I.J. Shon, J.K. Yoon, J.M. Doh, Consolidation of ultra fine WC and WC-Co hard materials by pulsed current activated sintering and its mechanical properties, Int. J. Refract. Met. Hard Mater. 25 (2007) 46–52.
[18] J.-E. Sundgren, T.G. Hentzel, A review of the present state of art in hard coatings grown from the vapor phase, J. Vac. Sci. Technol. A 4 (5) (1986) 2259–2279.
[19] S. Carvalho, E. Ribeiro, L. Rebouta, J. Pacaud, Ph. Goudeau, P.O. Renault, J.P. Rivière, C.J. Tavares, PVD grown (Ti,Si,Al)N nanocomposite coatings and (Ti,Al)N/(Ti,Si)N multilayers: structural and mechanical properties, Surf. Coat. Technol. 172 (2003) 109–116.
[20] J.V. Fernandes, A.C. Trindade, L.F. Menezes, A. Cavaleiro, Surf. Coat. Technol. 131 (2000) 457–461.
[21] J.M. Antunes, A. Cavaleiro, L.F. Menezes, M.I.J.V. Simões, Fernandes, ultra-microhardness testing procedure and Vickers indenter, Surf. Coat. Technol. 149 (2002) 27–35.
[22] N.M.G. Parreira, N.J.M. Carvalho, F. Vaz, A.1. Cavaleiro, Mechanical evaluation of unbiased W–O–N coatings deposited by dc reactive magnetron sputtering, Surf. Coat. Technol. 200 (2006) 6511–6516.
[23] G. Stoney, The tension of metallic films deposited by electrolysis, Proc. R. Soc. Lond. A 82 (1909) 172–175.
[24] F. Vaz, L. Rebouta, Ph. Goudeau, J.P. Rivière, E. Schäffer, G. Klee, M.1. Bodmann, Residual stress states in sputtered $Ti_{1-x}Si_xN_y$, Thin Solid Films 402 (2002) 195–202.
[25] S. Veprek, J.G. Maritza, Veprek-Heijman, Industrial applications of superhard nanocomposite coatings, Surf. Coat. Technol. 200 (2008) 5063–5073.
[26] S. Carvalho, L. Rebouta, A. Cavaleiro, L.A. Rocha, J. Gomes, E. Alves, Microstructure, Mechanical properties of nanocomposite (Ti,Si,Al)N coatings, Thin Solid Films 398–399 (2001) 391–396.
[27] S. Carvalho, Mechanical properties and microstructure of $Ti_{1-x-y}Si_xAl_yN$ nanocomposite thin films deposited by reactive magnetron sputtering, Ph.D. Thesis, Universidade do Minho, 2004 (in Portuguese).
[28] S. Carvalho, L. Rebouta, E. Ribeiro, F. Vaz, C.J. Tavares, E. Alves, N.P. Barradas, J.P. Riviere, Structural evolution of Ti–Al–Si–N nanocomposite coatings, Vacuum 83 (2009) 1206–1212.
[29] S. Veprek, H.-D. Männling, M. Yilek, P. Holubar, Avoiding high-temperature decomposition and softening of $(Al_{1-x}Ti_x)N/a\text{-}Si_3N_4$ nanocomposite, Mater. Sci. Eng. A 366 (2004) 202–205.
[30] R.F. Zhang, S. Veprek, Phase stabilities of self-organized nc-TiN/a-Si_3N_4 nanocomposites and of $Ti_{1-x}Si_xN_y$ solid solutions studied by ab initio calculation and thermodynamic modelling, Thin Solid Films 516 (2008) 2264–2275.
[31] J. Patscheider, Nanocomposite hard coatings for wear protection, MRS Bull. 28 (2003) 180.
[32] P. Holubar, M. Jilek, M. Sima, Present and possible future applications of superhard nanocomposite coatings, Surf. Coat. Technol. 133–134 (2000) 145–151.
[33] S. Veprek, M.G.J. Veprek-Heijman, R. Zhang, Chemistry, physics and fracture mechanics in search for superhard materials, and the origin of superhardness in nc-TiN/a-Si_3N_4 and related nanocomposites, J. Phys. Chem. Solids 68 (2007) 1161–1168.
[34] P.H. Mayrhofer, A. Hörling, L. Karlsson, J. Sjölén, T. Larsson, C. Mitterer, L. Hultman, Self-organized nanostructures in Ti–Al–N system, Appl. Phys. Lett. 83 (10) (2003) 2049–2051.
[35] S. Veprěk, P. Karvankova, M.G.J. Veprěk-Heijman, Possible role of oxugen impurities in degradation of nc-TiN/a-Si_3N_4 nanocomposite, J. Vac. Sci. Technol. B23 (6) (2005) L17.
[36] Peer Hendenqvist, Staffan Jacobson, Sture Hogmark, Tribological PVD coatings – characterisation of mechanical properties, Surf. Coat. Technol. 97 (1997) 212–217.
[37] R.F. Brito, S.R. de Carvalho, S.M.M.L. e Silva, J.R. Ferreira, Thermal analysis in coated cutting tools, Int. Com. Heat Mass Tranfer. 36 (2009) 314–321.
[38] A. Leyland, A. Matthews, On significance of the H/E ratio in wear control: a nanocomposite coatng approach to optimized tribological behavior, Wear 246 (2000) 1–11.
[39] N.M. Renevier, J. Hampshire, V.C. Fox, J. Witts, T. Allen, D.G. Teer, Advantages of using self-lubricating, hard, wear-resistant MoS_2-based coatings, Surf. Coat. Techol. 142–144 (2001) 67–77.
[40] A. Nossa, A. Cavaleiro, Mechanical behaviour of W–S–N and W–S–C sputtered coatings deposited with a Ti interlayer, Surf. Coat. Technol. 163–164 (2003) 552–560.
[41] F. Vaz, L. Rebouta, M. Andritscky, M.F. da Silva, J.C. Soares, Oxidation resistance of (Ti.Al,Si)N coatings in air, Surf. Coat. Technol. 98 (1998) 912–917.
[42] F. Vaz, L. Rebouta, M.F. da Silva, J.C. Soares, Thermal oxidation of ternary and quaternary nitrides of titanium, aluminium and silicon, in: Y. Pauleau, P. Barnas (Eds.), Protective Coatings and Thin Films: Synthesis, Characterization and Applications NATO Advanced Science Institutes series, Sub-series 3, High Tecnhology, Kluwer Acad. Publ., Dordrecht, 1996, pp. 501–510.
[43] Y. Tanaka, N. Ychimiya, Y. Onishi, Y. Yamada, Structure and properties of Al–Ti–Si–N coatings prepared by cathodic arc ion plating method for high speed cutting applications, Surf. Coat. Technol. 146–147 (2001) 215–221.
[44] A. Skopp, M. Woydt, K.-H. Habig, Tribological behavior of silicon nitride materials under unlubricated sliding between 22 °C and 1000 °C, Wear 181–183 (1995) 571–580.
[45] M. Woydt, A. Skopp, I. Dörfel, K. Witke, Wear engineering oxides/anti-wear oxides, Wear 218 (1998) 84–95.
[46] D. Ma, S. Ma, H. Dong, K. Xu, T. Bell, Microstruture and tribological behaviour of super-hard Ti–Si–C–N nanocomposite coatings deposited by plasma enhanced chemical vapour deposition, Thin Solid Films 496 (2006) 438–444.